This is a draft version. Please cite this paper as: Zheng, Z., Ahn, S., Chen, D., Laval, J., 2013. The effects of lane-changing on the immediate follower : anticipation, relaxation, and change in driver characteristics. Transportation Research Part C 26, 367-379.

The effects of lane-changing on the immediate follower: anticipation, relaxation, and change in driver characteristics

By
Zuduo Zheng[a] , Soyoung Ahn[b,*], Danjue Chen[c], Jorge Laval[c]

[a] Queensland University of Technology, 2 George St GPO Box 2434, Brisbane Qld 4001 Australia
[b] Arizona State University, P.O. Box 875306, Tempe, AZ 85287, U.S.A.
[c] Georgia Institute of Technology,790 Atlantic Dr. Atlanta, GA 30332-0355, U.S.A.

Abstract: This paper investigates the effects of lane-changing in driver behavior by measuring (i) the induced transient, non-equilibrium behavior and (ii) the change in driver characteristics, i.e., changes in driver response time and minimum spacing. We find that the transition largely consists of a pre-insertion transition and a relaxation process. These two processes are different but can be reasonably captured with a single model. Our findings also suggest that lane-changing induces a regressive effect on driver characteristics: a timid driver (characterized by larger response time and minimum spacing) tends to become less timid and an aggressive driver less aggressive. We offer an extension to Newell's car-following model to describe this regressive effect and verify it using vehicle trajectory data.

Key words: Lane-changing; Driver behavior; Car-following; Transition

1 Introduction

Vehicle lane-changing (LC) on freeways has received increasing attention due to their negative effects on bottleneck discharge rate. For instance, Cassidy and Rudjanakanoknad (2005) showed that when traffic density immediately upstream of a busy merge increases beyond a critical value, vehicles start to maneuver toward faster lanes, thereby causing traffic breakdown and "capacity drop". Laval and Daganzo (2006) postulated that this reduction occurs because lane-changers create voids in traffic streams due to bounded vehicle acceleration. They developed a multi-lane extension of the kinematic wave model (Lighthill and Whitham, 1955; Richards, 1956) by assuming each lane as a separate kinematic wave stream and treating lane-changers as particles with realistic mechanical properties. They showed that the model is able to replicate the observation by Cassidy and Rudjanakanoknad as well as the capacity of moving bottlenecks (Muñoz and Daganzo, 2002). Menendez and Daganzo (2007) enhanced this framework by considering a deceleration process before an insertion.

LC has also been linked to stop-and-go oscillations. Mauch and Cassidy (2002) found a strong correlation between the evolution of oscillations and LC in moderately dense queues; oscillations tended to form and grow near freeway interchanges where systematic LC maneuvers abounded. Kerner and Rehborn (1996) reported a similar finding. Ahn and Cassidy (2007) discovered using vehicle trajectory data that LC can trigger oscillations to form and grow in space. Zheng et al. (2011) further showed that LC is a primary trigger of oscillations in the absence of other exogenous factors (e.g., rubber-necking, noticeable vertical or horizontal curves). Moreover, they found that LC is primarily responsible for transforming subtle, localized oscillations to substantial disturbances.

In light of the important implications of LC, several studies examined its microscopic features, particularly the transition process during a LC maneuver. This transition process arises as the (equilibrium) car-following (CF) modes of a lane-changer and the immediate follower are disrupted due

to LC and then recovered gradually in time. Smith (1985) first reported that the transition typically persists for 25 seconds. Wang and Coifman (2008) and Ma and Ahn (2008) reported similar findings. They further showed that CF behavior is described well by Newell's simple CF model (Newell, 2002) except during the LC-induced transition period.

Laval and Leclercq (2008) proposed a microscopic framework of Laval and Daganzo (2006) to model this transition. Specifically, the microscopic model incorporates the relaxation phenomenon that arises as a lane-changer (or a follower) initially accepts a short spacing upon a maneuver and then gradually returns (relaxes) to a normal spacing given the speed. The model introduces only one additional parameter: the speed difference that the lane-changer is willing to accept during relaxation (ε). It was found that the model agrees well with macroscopic observations, such as the reduction in bottleneck discharge rate, and microscopic observations, such as individual vehicle trajectories (Leclercq et al., 2007). To facilitate more straightforward calibrations, Duret et al. (2011) reformulated the model by Laval and Leclercq using microscopic variables, such as the maximum passing rate, that can be readily measured and calibrated.

The above studies, however, describe the transition process after a lane-changer appears in the target lane. It is further assumed that the lane-changer (or the follower) revert to his/her behavior before LC, as per Newell's premise (Newell, 2002) that the driver characteristics are constant for each driver, independent of time and speed. However, it is likely that the transition begins while the lane-changer initiates a maneuver in the original lane. We refer to this as an "anticipation" period in this paper. Moreover, we conjecture that a follower may adapt her behavior at least temporarily after experiencing LC, perhaps in an effort to prevent another maneuver ahead.

In the present paper, we analyze (i) the entire transition period, consisting of anticipation and relaxation and (ii) change in driver characteristics due to LC. To facilitate this, we develop a method to systematically identify the beginning and end of the transition induced by LC and measure its ensuing impact on driver characteristic in terms of the response time and minimum spacing. The result suggests that the anticipation process is significant and (somewhat) different from the relaxation process. However, the existing relaxation model can describe both processes with reasonable accuracy. More importantly, we show strong evidence that LC can change driver characteristics (possibly temporarily) and propose an extended framework of Newell's CF model to capture this change.

This paper is organized as follows. Section 2 describes the study sites and data used in this research. Section 3 describes the methodology to identify the transition period of a follower during LC. Section 4 presents measurements of the transition process and the calibration result of applying Duret et al. model. Section 5 describes the analysis of time-dependent driver characteristics induced by LC and subsequent modeling efforts. Finally, Section 6 summarizes our findings and discusses future research.

2 Study sites and data

This study employs vehicle trajectory data available from FHWA's Next Generation Simulation (NGSIM) program (FHWA, 2008). These data were extracted from video images of northbound traffic on I-80 in Emeryville, California, and southbound traffic on US-101 in Los Angeles, California. The study site on I-80 is approximately 500 m, as shown in Figure 1(a). On this study segment, vehicle positions were recorded every 0.1 s from 4:00 p.m. to 4:15 p.m. and from 5:00 p.m. to 5:30 p.m. on April 13, 2005. The study site on US-101 is approximately 640 m, as shown in Figure 1(b), and trajectories on this study segment were collected from 7:50 a.m. to 8:35 a.m. on June 15, 2005. Lane numbers are incremented from the left-most lane. Each study site contains an on-ramp and an off-ramp, where many systematic

lane-changing activities are expected. The HOV lane on I-80 and the auxiliary lane on US-101 were excluded from the analysis because driving behavior in these lanes is likely different from that in the other lanes. Speed is estimated based on vehicle positions every 0.1 s and filtered using the simple weighted moving-average filter. Further, two types of noise in the data were removed: 1) any speed greater than 30 m/s (because traffic during the study periods was congested) and 2) LC maneuvers that lasted less than 5 s (Thiemann et al., 2008).

Figure 1

3 Methodology

This section describes the methodology to identify a transition state during LC. We first summarize Newell's simplified CF theory (Newell, 2002) because it forms the basis of our methodology.

3.1 Newell's simplified car-following model

Newell's CF model (see Figure 2) is appealing because it is parsimonious with only two parameters and gives the exact solution of the kinematic wave model with a triangular fundamental diagram (Daganzo, 2005). In this model, the trajectory of a vehicle in congested traffic on a homogenous highway is identical to the preceding vehicle's trajectory except for shifts in space and time. Suppose that vehicle $n-1$ initially travels at speed v and accelerates to v' due to a change in traffic conditions. Its trajectory, $x_{n-1}(t)$, can be approximated as a piecewise linear function defined by two constant speeds, v and v'. Then, according to Newell's theory, the follower, vehicle n, continues to travel at v until its spacing $x_{n-1}(t) - x_n(t)$ becomes sufficiently large and then accelerates to v'. As a result, vehicle n's trajectory is identical to vehicle $(n-1)$'s with a time shift τ_n and a space shift d_n. Thus, τ_n represents the duration that vehicle *n* waits until it accelerates (we refer to this as the response time), and d_n represents the minimum (or jam) spacing. Newell further conjectured that spacing $x_{n-1}(t) - x_n(t)$ at time t should remain nearly constant at some value s_n as long as the leader maintains a constant speed and that s_n solely depends on v for a single vehicle.

Figure 2

Newell further proposed that (τ_n, d_n) may vary from vehicle to vehicle as if they were sampled independently from some joint probability distribution, but they are constant and independent of speed for each driver. Several studies have provided empirical evidence in support of the theory (Ahn et al., 2004; Chiabaut et al., 2008; Duret et al., 2008; Ma and Ahn, 2008; Wang and Coifman, 2008).

3.2 Identification of the transition period induced by lane-changing

We measure the impact of a LC maneuver on the immediate follower in four regions illustrated in Figure 3. Region 1 is characterized by steady-state CF behavior prior to the insertion. Regions 2 and 3 comprise the LC-induced transition period. In region 2, the follower (vehicle 3) slows down prior to the insertion of vehicle 2, presumably to provide sufficient insertion space. Region 3 is characterized by relaxation to reach a larger spacing with the new leader, vehicle 2. Conceptually, we treat regions 2 and 3 differently because the follower may behave in response to both the lane-changer and the initial leader during the anticipation period, whereas his/her behavior during the relaxation period is affected by the new leader (lane-changer) only. (The result in Section 4.3 will show that these two processes are indeed

different, but the difference is reasonably small, such that the two processes may be treated as a single transition process.) For the moment, we separate these regions and categorize region 2 as an anticipation period. Finally, region 4 represents a post-relaxation state in which a change in CF characteristics may be observed in vehicle 3. Indeed we find that the driver characteristics in region 4 differ from that in region 1, indicating that a disturbance such as LC induces a change in driver characteristics. (A detailed analysis of this will follow in Section 5.)

Figure 3

To systematically identify the LC-induced transition period, the starting point of anticipation (p_1), the starting point of relaxation (p_2), and the ending point of relaxation (p_3) are first determined using Newell's CF theory. This is also illustrated in Figure 3, where τ_1 and d_1 are calculated using the trajectories of vehicle 1 and vehicle 3 before vehicle 2's insertion, and τ_2 and d_2 are calculated using the trajectories of vehicle 2 and vehicle 3 after vehicle 2's insertion. Parameters τ_1 and d_1 (and τ_2 and d_2) are selected in a way that the correlation between the two trajectories is maximized. Note that we relax Newell's assumption of constant τ and d for each driver by estimating two possibly-different sets of parameters before and after an insertion. Also note that vehicle 3's trajectory around the insertion represents a transition period and thus should be excluded in the parameter estimations. Based on Ma and Ahn (2008)'s preliminary finding that the impact of LC normally lasts less than 30 s, the trajectory within 15 s around the insertion is excluded.

A theoretical trajectory of vehicle 3, if vehicle 2 had not inserted, is obtained by shifting vehicle 1's trajectory by τ_1 and d_1 (the dashed line before vehicle 2's insertion in Figure 3). The actual trajectory starts to deviate from this theoretical trajectory at p_1 because vehicle 3 presumably slows down in anticipation of vehicle 2's insertion. Thus, p_1 is taken as the starting point of anticipation. Similarly, the theoretical trajectory of vehicle 3 (the dotted line in Figure 3) after vehicle 2's insertion is constructed by shifting vehicle 2's trajectory by τ_2 in time and d_2 in space. The convergence point between the theoretical and actual trajectories of vehicle 3 is the end point of relaxation (p_3). The divergence and convergence are determined based on a threshold of 2.3 m, which corresponds to approximately a half of the average vehicle length. Note that p_2, which is the time of the insertion (i.e., the time that vehicle 2 is first recorded in the target lane), is taken as the start of relaxation. The duration of anticipation (relaxation) is thus the time interval between p_1 and p_2 (p_2 and p_3).

In the NGSIM dataset, the "time of insertion" corresponds to the time when the front center of the vehicle crosses the edge of the target lane (NGSIM 2012). There are two sources of uncertainty with this time: (i) measurement error associated with the lateral coordinates of (the front center of) vehicles and (ii) ambiguity in equating the insertion time as the end of anticipation (and the start of relaxation). For instance, the shift from the anticipation to relaxation processes may occur in reality before or after the insertion point defined in the NGSIM data. Further, the shift may not be instantaneous. To address this, we rely heavily on statistical techniques and draw conclusions based on statistical significance. Our result shows that the shift from anticipation to relaxation turns out to be sufficiently short (2-3 s) and that the insertion time provided in the NGSIM data is a pretty good proxy for marking the shift. (The related result will be presented in Section 4.3.)

Finally, according to Newell's CF theory, (τ_1, d_1) should be the same as (τ_2, d_2) because τ and d are assumed to be constant for each vehicle independent of speed. Thus, the shifted vehicle 2 trajectory based on τ_1 and d_1 (the dash-dotted line in Figure 3) should be the same as the trajectory (the dotted line in

Figure 3) obtained based on τ_2 and d_2 if vehicle 3's behavior does not change. In contrast, a significant difference between the two theoretical trajectories indicates a change in driver characteristics (which we found to be prevalent).

4 Observation and modeling of lane-changing induced transition

4.1 Duration of transition period

Using the methodology described above, the anticipation and the relaxation periods induced by LC are measured using the trajectory data described in Section 2. Lane-changers in the dataset were filtered based on the criterion that the leader and the follower in regions 1 and 3 (see Figure 3) are observed for more than 10 s to estimate (τ_1, d_1) and (τ_2, d_2), respectively. We have analyzed 91 cases for I-80 and 86 cases for US-101. Figure 4 shows a typical example on I-80. In this figure, the estimated (τ_1, d_1) and (τ_2, d_2) are respectively (4.0 s, 4.5 m) and (4.0 s, 9.51 m).

Figure 4

Table 1 summarizes the durations of the transition period observed on I-80 and US-101. The anticipation and relaxation processes respectively persist for 6 – 14 s and 8 – 15 s on average with variations across sites and lanes. Overall, the anticipation durations are smaller than the relaxation durations at both sites; however, they are significant and hence should be considered in LC modeling. Of note, the duration of anticipation in lane 6 (shoulder lane on I-80) is a lot smaller compared to other lane, which may be attributable to merging vehicles. Finally, the duration of the entire transition period, particularly the duration of relaxation, tends to be site-specific as US-101 exhibits large values consistently across the lanes. This may be attributable to the fact that the US-101 site was less congested, although other factors such as grade may also affect the transition duration.

Table 1

4.2 Model

As mentioned in Section 1, the relaxation processes have been successfully modeled by Laval and Leclercq (2008) and reformulated by Duret et al. (2011) for a more straightforward calibration. In this section, the reformulated relaxation model by Duret et al. is extended to describe the entire transition process (including anticipation and relaxation processes) with a single set of parameters. Our motivation for using the same model is to preserve parsimony if the error is reasonably small.

In Duret et al. (2011), a lane-changer is initially in a non-equilibrium condition when appearing in the target lane and then gradually converges to Newell's CF equilibrium. This relaxation process is modeled using the maximum passing rate with the logic that the passing rate would temporarily deviate from an equilibrium rate during relaxation and then gradually converges to the equilibrium value. The maximum passing rate has been used in several previous studies (e.g., Daganzo, 2005; Chiabaut et al., 2009) because it is continuous in time and space and can be easily measured and calibrated. Furthermore, the maximum passing rate is closely related to Newell's CF theory (Newell, 2002) because τ is the reciprocal of the maximum passing rate. For our analysis, we use the formulation in τ to be consistent with other analyses. The mathematical formulation is

$$\tau^{i+1}(t) = \tau^{i+1}(0) + \frac{\varepsilon}{\beta} ln\left(1 + \frac{\beta t}{w + v^i(0)}\right) \quad (1)$$

where $\tau^{i+1}(t)$ is the response time of vehicle $i+1$ at time t; $\tau^{i+1}(0)$ is the initial response time of vehicle $i+1$; ε is the speed difference vehicle $i+1$ is willing to accept; β is a constant acceleration rate of the lead vehicle; $v^i(0)$ is the initial speed of vehicle i and w is the average speed of kinematic waves. In applying the model, t is finite because once a driver reaches a steady-state (i.e., once τ reaches an equilibrium value), the driver will follow Newell's car-following principle. For this model, only one parameter, ε, needs to be calibrated while the others can be measured directly from observations. Note that to keep the model efficient, all parameters are obtained using the average values across vehicles.

In extending the above model to predict the anticipation process, one needs to determine whether to measure τ's with respect to the leader in the same lane or the lane-changer in the initial lane prior to insertion. Our preliminary analysis shows that the follower's behavior is more correlated to the lane-changer's behavior in the initial lane rather than the leader in the same lane. Thus, the calibration of the model is performed by measuring τ's between a lane-changer and the follower.

4.3 Model calibration

As illustrated in Figure 5, τ's are measured along a set of kinematic waves propagating backwards in space at speed w. In the figure, the dashed line is the trajectory of the lane-changer in the initial lane during the anticipation. The lane-changer (vehicle i) signals its lane-changing intention at time ${t_0}^i$, thereby emanating the first kinematic wave. This wave arrives at vehicle $i+1$ at ${t_0}^{i+1}$ and initiates an anticipation process (marked as p_1 in the figure). Then, τ along the first wave is computed as $({t_0}^{i+1} - {t_0}^i)$. Similarly, τ's are measured along successive waves to capture the dynamic processes of LC-induced transition. In this study, τ is measured every second. As we assume that parameters τ and d can change after a LC maneuver, wave speed ($=d/\tau$) may also change. However, a statistical test (two sample *t*-test) result shows that the wave speed does not change significantly for both lane-changers and followers, indicating that τ and d tend to change proportionally in the same direction.

Calibration was performed on 70 cases out of 91 for I-80. Other 21 cases did not yield long enough trajectories (in equilibrium) of lane-changers in the initial lanes because the lane-changers made successive maneuvers or their behavior was affected by other lane-changing maneuvers ahead. US-101 is not used for calibration because of a small sample size (less than 10).

Figure 5

For parameters w, $v^i(0)$, and β, we use the same values as in Duret et al. (2011) because the same NGSIM datasets are used; w = 5 m/s, $v^i(0)$ = 5 m/s, and β = 2.08 m/s^2. Then we calibrate $\tau^{i+1}(0)$ and ε simultaneously by minimizing the root mean squared error (RMSE) between observed and predicted τ values. The calibrated value of $\tau^{i+1}(0)$ is 0.47 s with confidence interval (CI) of (0.44, 0.51). The calibrated value of ε is 0.74 m/s with CI of (0.7, 0.77). The RMSE and the mean absolute percentage error (MAPE) are respectively 0.05 and 3.7%, demonstrating a good calibration performance. Figure 6 shows the temporal evolution of observed values of τ (solid circles) against the estimated values by the model (solid curve). (Note that the observed values represent the average across all 70 cases. It is notable that the transition from anticipation to relaxation is not instantaneous but sufficiently short (2-3 seconds) and that the insertion time provided in the NGSIM data is a pretty good proxy for marking the transition. Further,

the estimated values of τ fit the observed values reasonably well, though larger deviations are observed during the anticipation period. The absolute percentage errors shown in Figure 7 confirm this observation. The absolute percentage error tends to be larger during anticipation with the maximum of around 12%, indicating that the model performance is inferior during anticipation. This can be remedied by using a different set of parameters during anticipation. However, the performance is still reasonable, and a single set of parameters may suffice for the sake of preserving parsimony.

Figure 6

Figure 7

5 Time-dependent driver characteristics

5.1 Observation

As described in Section 3, (τ_1, d_1) and (τ_2, d_2) should be similar if the driver behavior before and after LC remains unchanged. Our analysis reveals that this is often not the case (see Figure 4, where the values of d_1 and d_2 are very different). We observed numerous cases of such changes in driver characteristics with varying degrees. However, the ratio of the parameters (i.e., wave speed, d/τ) did not change significantly, though some variations are expected at the individual vehicle level (as in Figure 4).

To further investigate the changes in driver characteristics, the changes (i.e., $\tau_2 - \tau_1$ and $d_2 - d_1$) are plotted against the amount of deviation from "average" driving behavior before LC (i.e., $\tau_1 - \bar{\tau}$ and $d_1 - \bar{d}$), where $\bar{\tau}$ and $\bar{d}$ are average values of τ and d prior to LC. As shown in Figure 8, these plots reveal seemingly linear trends with negative slopes. (We show the plots for the followers at US-101 as representative examples.) The trends imply that a driver with τ larger (smaller) than $\bar{\tau}$ adjusts her driving by reducing (increasing) τ after LC. The same interpretation applies to d. We characterize a driver as "timid" if $\tau_1 > \bar{\tau}$ and/or $d_1 > \bar{d}$. A driver is characterized as "aggressive" if $\tau_1 < \bar{\tau}$ and/or $d_1 < \bar{d}$. Note that the trajectory of a timid (aggressive) driver would lie below (above) the trajectory of an average driver. (This convention is consistent with Laval and Leclercq (2010).) Using $\bar{\tau}$ and $\bar{d}$ offers a straightforward and robust way to distinguish timid vs. aggressive drivers since (i) it is derived from Newell's CF model and thus maintains the theoretical consistency with other analyses in our study; and (ii) it is not sensitive to the individual measurement errors and consistent across sites (2.0 s and 2.2 s for τ and 5.4 m for d, respectively for I-80 and US-101).

Figure 8

Finally, we examine the effect of a lane-changer's characteristics on the follower's characteristics to help formulate a basic model for the change in driver behavior. Specifically we examine three relationships: (i) $\tau_{2,f}$ vs. $\tau_{2,l}$, (ii) $\left(\tau_{2,f} - \tau_{1,f}\right)$ vs. $\tau_{2,l}$, and (i) $\left(\tau_{2,f} - \tau_{1,f}\right)$ vs. $\left(\tau_{2,l} - \tau_{1,l}\right)$, where subscript f (l) represents follower (lane-changer). The first relationship examines the correlation between a lane-changer and a follower in terms of aggressiveness after LC; the second examines the change in the follower's characteristics in relation to the lane-changer's aggressiveness; the third examines the correlation in terms of change in driver characteristics. As the results in Figure 9 show, no significant correlations are found for all three relationships. (The results based on parameter d were similar.) This implies that a follower's characteristics and any changes therein are related to her own behavior and

independent of the leader's behavior. This finding facilitates a simpler formulation of the change in driver characteristics, as reflected in our modeling structure in the following section.

Figure 9

5.2 Model

In this section, we develop a model to predict the extent of change in characteristics for individual drivers measured by time-dependent τ and d. We postulate that the extent of a change in driver characteristics, (i.e., $\tau_2 - \tau_1$ and $d_2 - d_1$) depends on the amount of deviation from "average" driving behavior before LC (i.e., $\tau_1 - \bar{\tau}$ and $d_1 - \bar{d}$). We assume that the average values of τ and d prior to LC represent *average* driving behavior. Table 2 reports the sample size and the average values computed separately for lane-changers and followers at each site. Notably the values of τ and d are similar between sites, although τ values are smaller for lane-changers.

Table 2

Of note, half of the follower sample (Dataset I hereafter) from each site is used to develop models, and the other half (Dataset II hereafter) is reserved for later model validation. However, the sample for lane-changers is not divided to maintain sufficient sample size for model estimation.

Without loss of generality, the relationship between $(\tau_2 - \tau_1)$ and $(\tau_1 - \bar{\tau})$ is expressed as

$$\tau_2 - \tau_1 = \alpha(\tau_1 - \bar{\tau}) + \beta. \qquad (2)$$

Table 3 summarizes the estimated parameters and supporting statistics for followers. Notably, all linear models are statistically significant at the 99 percent confidence level ($p < 0.01$), with R^2 ranging from 0.30 to 0.51. Considering that individual driving behavior is modeled, these R^2 values are quite reasonable. The constant terms are insignificant.

Table 3

To gain more insight on this relationship, Equation (2) is rearranged to obtain

$$\tau_2 - \bar{\tau} = (\alpha + 1)(\tau_1 - \bar{\tau}) + \beta. \qquad (3)$$

Based on the modeling results shown in Table 3, $-1 < \alpha < 0$ (or $0 < \alpha + 1 < 1$) and $\beta \approx 0$. Therefore, Equation (3) indicates that the deviation of τ from the average driving behavior becomes smaller after experiencing LC because $0 < \alpha + 1 < 1$. This relationship implies that a timid driver, who is characterized by $\tau_1 - \bar{\tau} > 0$, becomes less timid after experiencing LC ahead, though the driver remains timid because $\tau_2 - \bar{\tau} > 0$. Similarly, an aggressive driver remains aggressive after experiencing LC but becomes less aggressive.

The same results are obtained using d because the estimated coefficients based on d are similar to those based on τ. Thus, we can conclude that (i) the impact of LC on the immediate follower's driving behavior is not strong enough to convert a timid driver to an aggressive one or vice versa, and (ii) LC "neutralizes" the immediate follower's behavior by encouraging a timid (aggressive) driver to become less timid (aggressive).

Table 4 shows the estimation results for lane-changers. The results are similar to those for followers: all linear models are statistically significant with R^2 values ranging from 0.50 to 0.74; the estimated α

values are between –1 and 0, although they are closer to –1. An exception is that the constant term, β, is sometimes significant, indicating that a regressive effect for lane-changers is not as apparent. This is not surprising since a lane-changer creates a disturbance in traffic stream and induces regressive effect for followers.

Table 4

5.3 Model validation

We use Dataset II from each site to validate the aforementioned findings. As a preliminary assessment, linear models are estimated and compared to the results based on Dataset I, as summarized in Table 5. The results show that the coefficients estimated on the basis of Dataset I are similar to those estimated on the basis of Dataset II. Moreover, all of the models are significant at the 99 percent confidence level, with R^2 ranging from 0.30 to 0.53. The constant terms are often insignificant.

Table 5

As a further validation, we cross-validate the models; i.e., the models based on one dataset are used to predict τ_2 and d_2 in the other dataset. As an example, Figure 10(a) shows the amount of prediction error in τ_2, which is calibrated using Dataset I and applied to Dataset II for I-80; approximately 60% of the predictions are within 0.5 s (about 40% error). Similarly, Figure 10(b) shows the amount of prediction error in τ_2 with the calibration and validation datasets switched; approximately 70% of predictions are within 0.5 s. A similar conclusion has been reached for d_2.

Figure 10

Table 6 shows the MAPEs for all cross-validation scenarios. The MAPE of τ_2 varies from 24% to 41%, which is consistently lower than d_2's MAPE. Although noticeable estimation errors exist, as reflected by relatively large MAPEs in Table 6 and the mid-ranged R^2 values in Table 5 the model performance is quite reasonable given large variations expected in individual driving behavior. Moreover, the model is parsimonious with a single variable (τ_1 or d_1), indicating that the model can be transferred to other locations with flexibility. One may develop a more complex model to decrease the errors, but it may increase the risk of over-fitting the data.

In addition, the table also shows that our extended model outperforms the original Newell's CF model; MAPEs of τ_2 and d_2 using Newell's model (i.e., assuming $\tau_2 = \tau_1$ and $d_2 = d_1$) are much larger than the counterparts of our extend model. It again confirms the necessity of incorporating time-dependent driver characteristics into Newell's CF model.

Table 6

5.4 Macroscopic implications

The macroscopic implication of the changes in driver characteristics due to LC can be seen in Figure 11, which shows the evolution of the average τ across all the sampled followers at each study site. Note that the τ values are calculated based on vehicles 1 and 3 during the anticipation process and based on

vehicles 2 and 3 during the relaxation process (see Figure 3 for vehicle reference). The average τ for I-80 during the equilibrium state before anticipation is stable at about 1.5 s (see Figure 11(a)); it changes over time during the anticipation and relaxation processes; then it eventually converges to another equilibrium state with τ of about 1.3 s after relaxation. The 13% decrease in equilibrium τ is statistically significant at a 0.05 level and implies systematic changes in driver behavior. Similarly, a change in driver characteristics on US-101 is characterized by 5.7% decrease in equilibrium passing rate (see Figure 11(b)). Although the amount of reduction is smaller for US-101, it is still statistically significant.

The same analysis for lane-changers at I-80 is shown in Figure 11(c). US-101 is not used for analyzing lane-changers because of a small sample size in steady states (less than 10). For a lane-changer, τ is measured every second with respect to a leader in the initial (target) lane during the anticipation (relaxation) periods. A 7.2% decrease in equilibrium τ is detected. The result is similar to those for the followers: the average τ converges to a different value after relaxation, indicating a systematic change in driver characteristics. Note that the systematic change in lane-changers' characteristics is attributed to LC itself rather than different overall behaviors between lanes; we find no significant differences in average driver characteristics between lanes in terms of τ, and d.

The results indicate that in general, drivers (a lane-changer or a follower) become more aggressive (smaller τ) after experiencing LC. Consistent with the modeling result in sections 5.2 and 5.3, this finding suggests that Newell's assumption of constant τ and d should be relaxed to capture time-dependent driver characteristics, especially around major disturbances such as LC.

Figure 11

6 Conclusions and future study

This study sheds light on the impacts of LC on the immediate follower in the target lane and offers simple models to capture such impacts. We provide a method to systematically identify different components of LC impact: (i) anticipation process, (ii) relaxation process, and (iii) change in driver characteristics induced by LC. Using the NGSIM vehicle trajectories, we found that the average durations for the anticipation and relaxation processes respectively range 8 – 14 s and 10 – 15 s, underlining that both components should be considered in assessing the LC impact. These two processes were found to be statistically different. However, the difference was small enough to model them as a single process using the relaxation model by Duret et al. (2011) and Laval and Leclercq (2008).

We also found that LC induces changes in driver characteristics. These changes were systematic and suggest that drivers tend to become more aggressive (characterized by smaller response time and minimum spacing) perhaps to prevent another LC maneuver. A simple statistical model is able to predict the extent of changes with reasonable accuracy. The modeling results suggest that (i) the magnitude of change is linearly related to the amount of deviation from the average driving behavior (across drivers) prior to LC; (ii) LC has a regressive effect, that is, a timid (aggressive) driver becomes less timid (aggressive) after experiencing LC; and (iii) LC is unlikely to convert a timid driver to an aggressive one and vice versa. This finding implies that Newell's conjecture of constant response time and minimum spacing for each vehicle should be relaxed to reflect time-dependent driver characteristics.

The above findings shed light on transient traffic and variable driver characteristics induced by LC, which will help better describe important traffic phenomena. For instance, LC is known to be a major factor for capacity drop. Thus, the LC-induced impact quantified in this study will be useful for estimating/predicting the amount of capacity drop with better accuracy. Further, incorporating variable

driver characteristics has the potential to reproduce growth or decay of disturbances as in Laval and Leclercq (2010) and Chen et al. (2012).

Nonetheless, future efforts are necessary to fully appreciate the impact of LC on traffic dynamics. For instance, we need a better understanding of the impact of a LC desertion in the initial lane and the propagation of a LC-induced disturbance (e.g., change in driver characteristics) to quantify the global impact of LC. The methodology developed in this paper can be applied to study these elements. Research in this regard is ongoing. It is also necessary to examine how long the changes in driver characteristics persist, if not permanent. Our study sites were not long enough to investigate this feature. Finally, it would be useful to investigate other potential factors for changes in driver characteristics to reduce prediction errors. However, we caution that an overly complex model may increase the risk of over-fitting the data as indicated in Punzo et al. (2005).

References

Ahn, S., Cassidy, M.J., 2007. Freeway traffic oscillations and vehicle lane-change maneuvers. In: Allsop, R.E., Bell, M.G.H., Heydecker, B. (Eds.), Proceedings of the 17th International Symposium on Transportation and Traffic Theory, Amsterdam, Elsevier, pp. 691-710.

Ahn, S., Cassidy, M.J., Laval, J.A., 2004. Verification of a simplified car-following theory. Transportation Research Part B 38 (5), 431-440.

Cassidy, M.J., Rudjanakanoknad, J., 2005. Increasing the capacity of an isolated merge by metering its on-ramp. Transportation Research Part B 39 (10), 896-913.

Chen, D., Laval, J., Zheng, Z., Ahn, S., 2012. Validation, improvement, and application of a parsimonious traffic oscillation model. In press. Transportation Research Part B.

Chiabaut, N., Buisson, C., Leclercq, L., 2009. Fundamental diagram estimation through passing rate measurements in congestion. IEEE Transactions on Intelligent Transportation Systems 10 (2), 355-359.

Chiabaut, N., Leclercq, L., Buisson, C., 2008. From heterogeneous drivers to macroscopic patterns in congestion. Transportation Research Part B 44 (2), 299-308.

Coifman, B., Mishalani, R., Wang, C., Krishnamurthy, S., 2006. Impact of lane-change maneuvers on congested freeway segment delays: Pilot study. Transportation Research Record 1965, 152-159.

Daganzo, C.F., 2005. A variational formulation of kinematic waves: basic theory and complex boundary conditions. Transportation Research Part B 39 (2), 187-196.

Duret, A., Ahn, S., Buisson, C., 2011. Passing rates to measure relaxation and impact of lane-changing in queue. Computer Aided Engineering and Infrastructure Engineering 26 (4), 285-297.

Duret, A., Chiabaut, N., Buisson, C., 2008. Estimating individual speed-spacing relationship and assessing ability of Newell's car following model to reproduce trajectories. Transportation Research Record: Journal of the Transportation Research Board 2088, 188-197.

FHWA. The next generation simulation (NGSIM). <http://www.ngsim.fhwa.dot.gov/> (05/08, 2008).

Kerner, B., Rehborn, H., 1996. Experimental features and characteristics of traffic jams. Physical Review E 53 (2), 1297-1300.

Laval, J.A., Leclercq, L., 2008. Microscopic modeling of the relaxation phenomenon using a macroscopic lane-changing model. Transportation Research Part B 42 (6), 511-522.

Laval, J.A., Daganzo, C.F., 2006. Lane-changing in traffic streams. Transportation Research Part B 40 (3), 251-264.

Leclercq, L., Chiabaut, N., Laval, J.A., Buisson, C., 2007. Relaxation phenomenon after changing lanes: an experimental validation with the NGSIM dataset. Transportation Research Record: Journal of the Transportation Research Board 1999, 79-85.

Lighthill, M., Whitham, G., 1955. On kinematic waves: II. A theory of traffic flow on long crowded roads. Proceedings of the Royal Society of London. Series A, Mathematical and Physical Sciences 229 (1178), 317-345.

Ma, T., Ahn, S., 2008. Comparisons of speed-spacing relations under general car following versus lane-changing. Transportation Research Record: Journal of the Transportation Research Board 2088, 138-147.

Mauch, M., Cassidy, M.J., 2002. Freeway traffic oscillations: Observations and predictions. In: Taylor, M.A.P. (Ed.), Proceedings of the15th International Symposium on Transportation and Traffic Theory. Pergamon-Elsevier, Oxford, UK, pp. 653–674.

Menendez, M., Daganzo, C.F., 2007. Effects of HOV lanes on freeway bottlenecks. Transportation Research Part B 41 (8), 809-822.

Muñoz, J.C., Daganzo, C.F., 2002. Moving bottlenecks: A theory grounded on experimental observation. In: Taylor, M.A.P. (Ed.), Proceedings of the 15th International Symposium on Transportation and Traffic Theory. Pergamon–Elsevier, Oxford, UK, pp. 441–462.

Newell, G.F., 2002. A simplified car-following theory: a lower order model. Transportation Research Part B 36 (3), 195-205.

Newell, G.F., 1993. A simplified theory of kinematic waves in highway traffic, part I: General theory. Transportation Research Part B 27 (4), 281-287.

NGSIM, Vehicle trajectory file data dictionary. http://ops.fhwa.dot.gov/trafficanalysistools/ngsim.htm (accessed on March 15, 2012).

Punzo, V., Simonelli, F., 2005. Analysis and comparison of microscopic traffic flow models with real traffic microscopic data. Transportation Research Record: Journal of the Transportation Research Board 1934, 53-63.

Richards, P.I., 1956. Shock waves on the highway. Operations Research 4 (1), 42-51.

Smith, S.A., 1985. Freeway data collection for studying vehicle interactions. Federal Highway Administration; Available through the National Technical Information Service.

Thiemann, C., Treiber, M., Kesting, A., 2008. Estimating acceleration and lane-changing dynamics based on NGSIM trajectory data. Transportation Research Record: Journal of the Transportation Research Board 2088, 90-101.

Wang, C. Coifman, B., 2008. The effect of lane-change maneuvers on a simplified car-following theory. IEEE Transactions on Intelligent Transportation Systems 9 (3), 523-535.

Zheng, Z., Ahn, S., Chen, D., Laval, J.A., 2011. Freeway traffic oscillations: microscopic analysis of formations and propagations using wavelet transform. Transportation Research Part B 45 (9), 1378-1388.

List of Tables

List of Figures

Figure

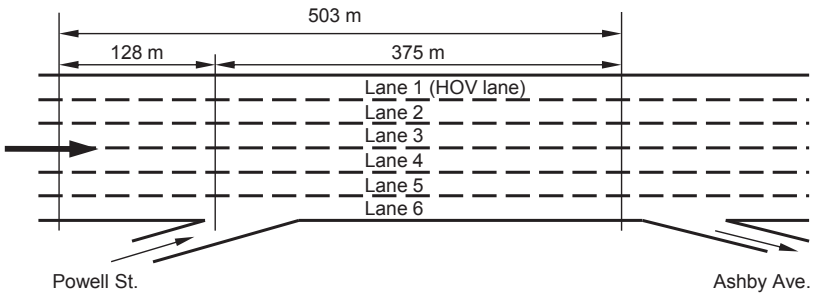

(a)

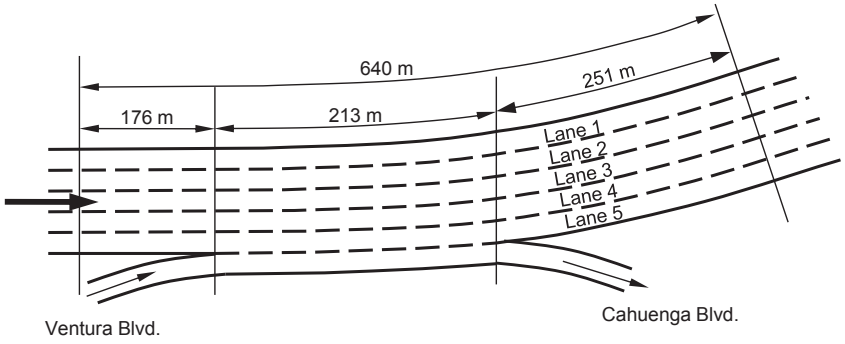

(b)

Figure 1 Schematic illustrations of study sites; (a) northbound I-80 in Emeryville, California; (b) southbound US-101 in Los Angeles, California; Lane numbering is incremented from the left-most lane.

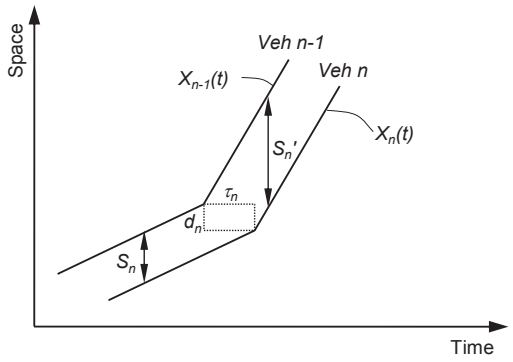

Figure 2 Illustration of Newell's car-following theory using vehicle trajectories (Newell, 2002).

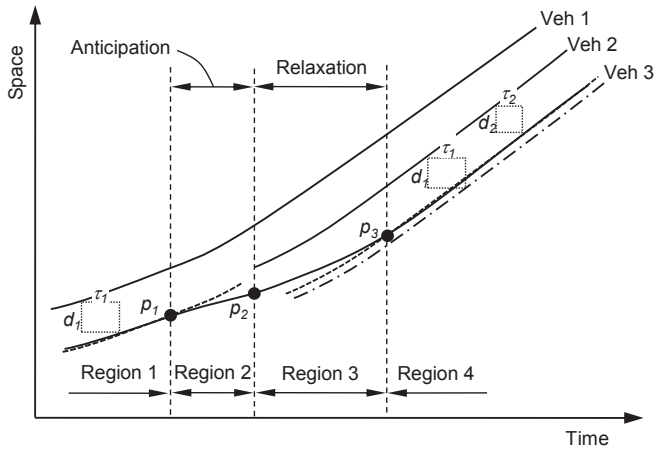

Figure 3 Three hypothetical vehicle trajectories to illustrate the identification of anticipation, relaxation, and change in driver characteristics based on Newell's CF theory; vehicle 1 (leader), vehicle 2 (lane changer), and vehicle 3 (follower).

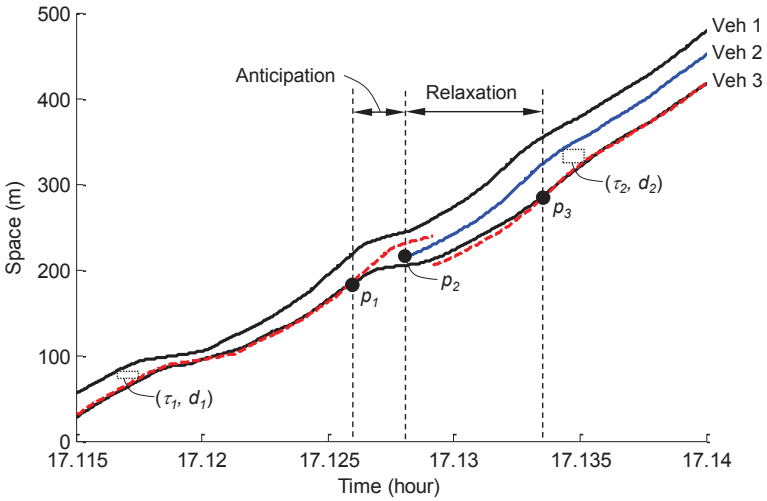

Figure 4 An example of identified anticipation and relaxation periods for a following vehicle (Veh 3); solid lines represent actual trajectories, and dashed lines represent theoretical trajectories.

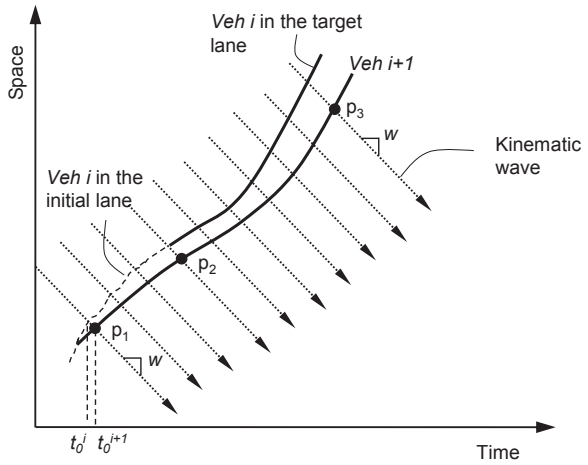

Figure 5 Illustration of measuring τ's along kinematic waves.

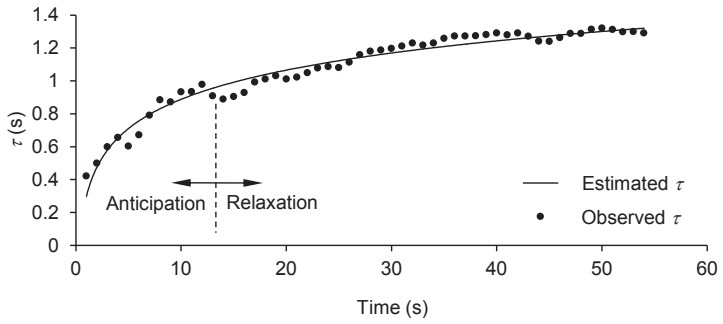

Figure 6 Temporal evolution of average τ's for all the followers, I-80; τ's are measured with respect to lane changers.

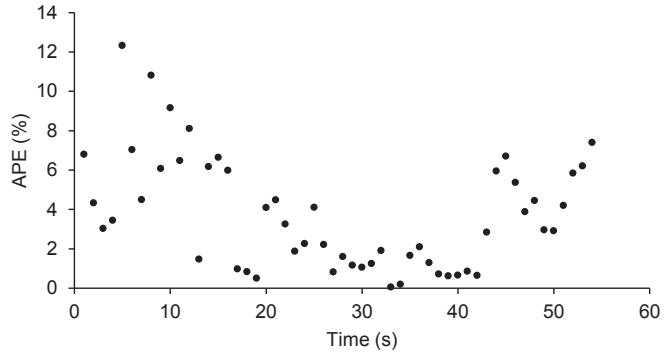

Figure 7 Model calibration result: absolute percentage errors (APE).

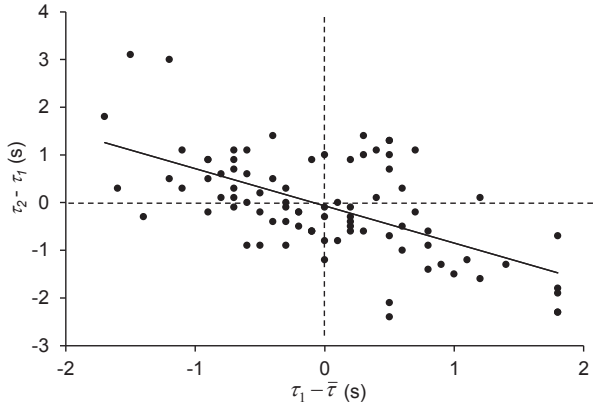

(a)

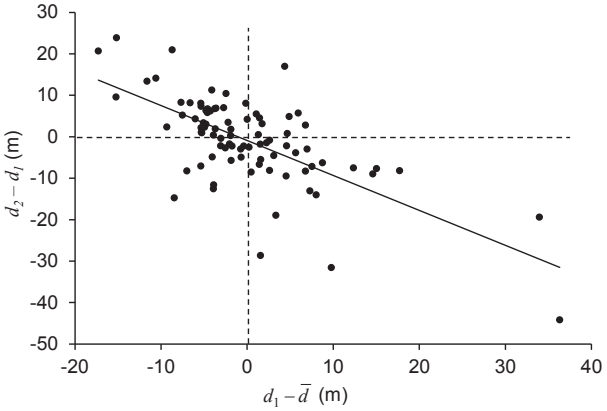

(b)

Figure 8 Change in driver characteristics vs. deviation from average driving behavior; (a) $\tau_2 - \tau_1$ vs. $\tau_1 - \bar{\tau}$ for followers, US-101; (b) $d_2 - d_1$ vs. $d_1 - \bar{d}$ for followers, US-101.

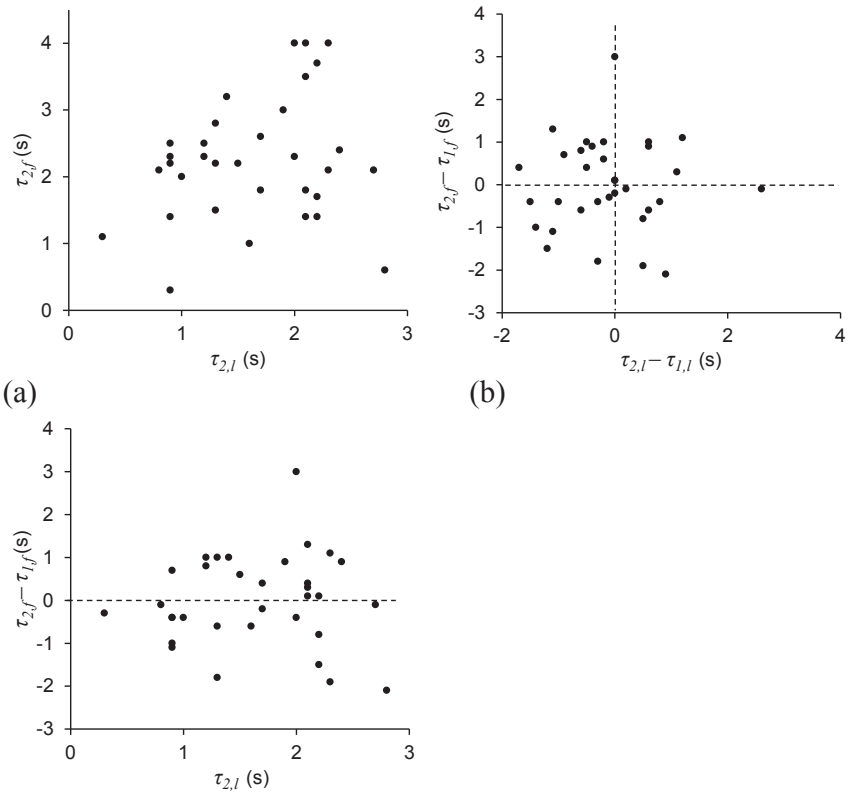

Figure 9 Relationships between characteristics of lane-changers and characteristics of followers at both study sites; (a) $\tau_{2,f}$ vs. $\tau_{2,l}$; (b) $(\tau_{2,f} - \tau_{1,f})$ vs. $\tau_{2,l}$; (c) $(\tau_{2,f} - \tau_{1,f})$ vs. $(\tau_{2,l} - \tau_{1,l})$.

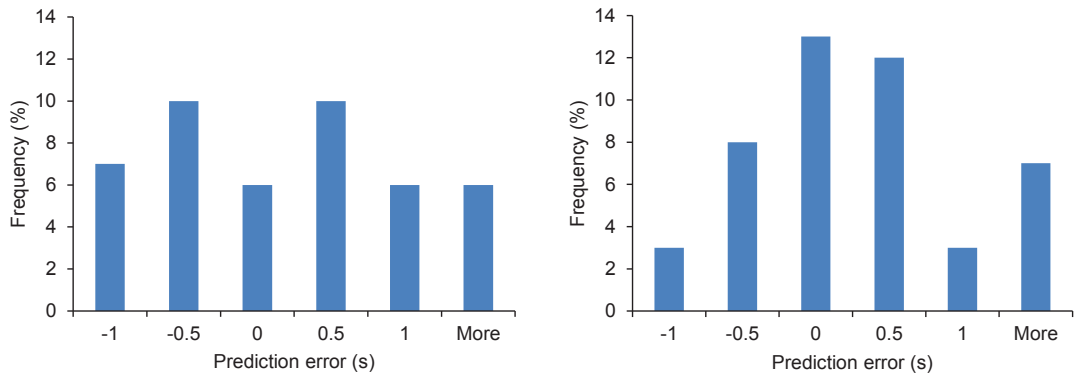

(a) (b)

Figure 10 Frequency distributions of prediction error in τ_2, I-80: (a) τ_2 calibrated using Dataset I and applied to Dataset II; (b) τ_2 calibrated using Dataset II and applied to Dataset I.

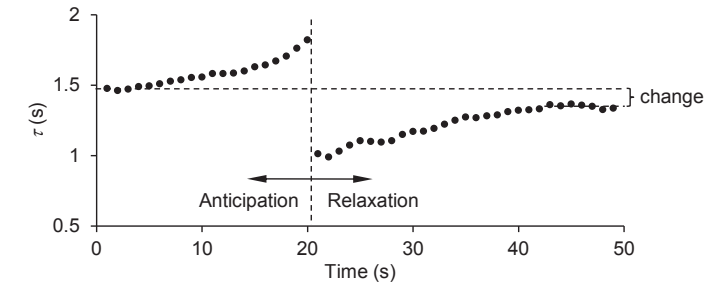

(a)

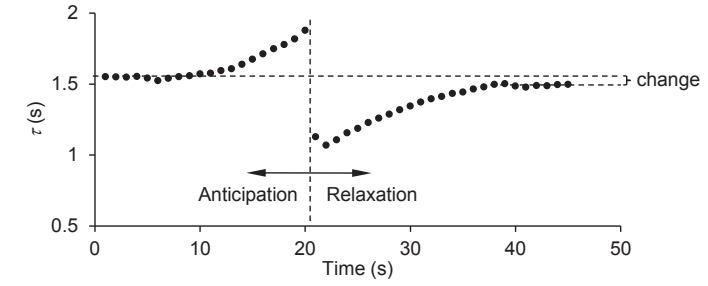

(b)

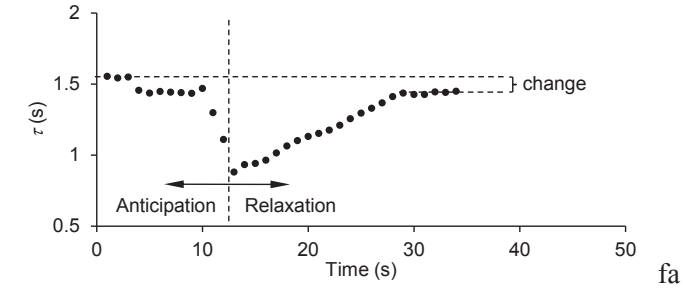

fa

(c)

Figure 11 Temporal evolution of average τ's; (a) I-80, followers; (b) US-101, followers; (c) I-80, lane-changers; τ's are measured with respect to the leaders in the same lane.

Table

Table 1 Summary statistics for the durations of anticipation and relaxation, τ, and d

I-80						
Lane ID	2	3	4	5	6	Total
Sample Size	13	12	6	11	49	91
Anticipation (s)	8.3 (2.2*)	10.2 (1.6)	8.8 (4.0)	12 (2.9)	5.9 (1.0)	7.8 (0.8)
Relaxation (s)	11.6 (2.9)	11.5 (2.6)	8.3 (4.0)	12.9 (2.7)	10.3 (1.5)	10.8 (1.1)
τ (s)	1.8 (0.24)	2.5 (0.34)	2.1 (0.31)	2.3 (0.26)	1.9 (0.14)	2.0 (0.1)
d (m)	7.2 (1.6)	4.5 (2.4)	6.2 (2.4)	5.5 (1.5)	5.7 (0.8)	5.4 (0.6)
US-101						
Lane ID	1	2	3	4	5	Total
Sample Size	8	18	14	24	22	86
Anticipation (s)	13.8 (4.1)	9.7 (1.8)	8.3 (2.0)	11.1 (1.5)	8.6 (1.4)	10 (0.8)
Relaxation (s)	14.9 (3.3)	13.4 (1.9)	14.9 (1.7)	13.6 (2.1)	12.7 (1.8)	13.7 (0.9)
τ (s)	2.5 (0.29)	2.5 (0.19)	2.3 (0.23)	2.1 (0.17)	2 (0.16)	2.2 (0.09)
d (m)	6.2 (2)	5.2 (1.4)	5.5 (2.1)	4.8 (2)	5.8 (2.1)	5.4 (0.9)

* the standard error

Table 2 Sample size, n, and average values of τ and d

Site	Variable	Lane changer	Immediate follower
I-80	n	43	91
	$\bar{\tau}\,(s)$	1.5	2.0
	$\bar{d}\,(m)$	5.6	5.4
US-101	n	48	86
	$\bar{\tau}\,(s)$	1.5	2.2
	$\bar{d}\,(m)$	4.6	5.4

Table 3 Summary of modeling results: followers using Dataset I

Site	Dependent Variable	Variable	Coefficient	p Value	Overall Goodness of Fit	
					p Value	R^2
I-80	$\tau_2 - \tau_1$	β	-0.0188	0.88	<.01	0.41
		α	-0.670	<.01		
	$d_2 - d_1$	β	-1.281	0.24	<.01	0.30
		α	-0.819	<.01		
US-101	$\tau_2 - \tau_1$	β	-0.0461	0.73	<.01	0.36
		α	-0.776	<.01		
	$d_2 - d_1$	β	-0.853	0.42	<.01	0.51
		α	-0.782	<.01		

Table 4 Summary of modeling results: lane-changers

Site	Dependent Variable	Variable	Coefficient	p Value	Overall Goodness of Fit	
					p Value	R^2
I-80	$\tau_2 - \tau_1$	β	-0.318	<.01	<.01	0.70
		α	-0.919	<.01		
	$d_2 - d_1$	β	0.914	0.14	<.01	0.64
		α	-0.951	<.01		
US-101	$\tau_2 - \tau_1$	β	0.113	0.10	<.01	0.51
		α	-0.776	<.01		
	$d_2 - d_1$	β	-1.790	<.01	<.01	0.50
		α	-0.824	<.01		

Table 5 Summary of modeling results: followers using Dataset II

Site	Dependent Variable	Variable	Coefficient	P	Overall Goodness of Fit	
					P	R^2
I-80	$\tau_2 - \tau_1$	β	-0.0617	0.67	<.01	0.38
		α	-0.780	<.01		
	$d_2 - d_1$	β	-0.250	0.12	<.01	0.30
		α	-0.778	<.01		
US-101	$\tau_2 - \tau_1$	β	-0.168	0.18	<.01	0.36
		α	-0.716	<.01		
	$d_2 - d_1$	β	-0.629	0.54	<.01	0.53
		α	-0.809	<.01		

Table 6 Summary of the validation results

I-80			US-101		
Calibration Dataset	Variable	MAPE	Calibration Dataset	Variable	MAPE
I	τ_2	41	I	τ_2	24
	d_2	59		d_2	59
II	τ_2	27	II	τ_2	32
	d_2	55		d_2	59
Newell's model	τ_2	77	Newell's model	τ_2	52
	d_2	207		d_2	173